

Data Dependent Jitter (DDJ) Characterization Methodology

Kyung Ki Kim, Yong-Bin Kim, Fabrizio Lombardi
Department of Electrical and Computer Engineering
Northeastern University, Boston, MA, USA
E-mail: kkkim@ece.neu.edu, ybk@ece.neu.edu, Lombardi@ece.neu.edu

Abstract

A new jitter model is developed using Matlab and Spice to analyze Data Dependent Jitter (DDJ) in serial data integrated circuits. The simulation results show that DDJ is dependent on the data pattern, data rate, and data slew as well as frequency bandwidth, impedance mismatch, and loss of the data path of integrated circuits. This paper presents the effect of the DDJ on other jitter subcomponents, which is essential to analysis and characterization of DDJ.

1. Introduction

As the data rate of a VLSI system increases, serial links between chips and even on chip become more significant in the system to require timing accuracy. Therefore, timing jitter modeling is required to analyze the high-speed serial data path.

Timing jitter (henceforth shortened to jitter) is defined as the deviation of a signal transition from its ideal position in time. The total jitter (TJ) is composed of the Random Jitter (RJ) and Deterministic Jitter (DJ). The RJ results from device noise sources such as flicker and thermal noise. This is theoretically unbounded in amplitude, and is theoretically characterized by Gaussian distribution, while the DJ consists of Duty-Cycle Distortion (DCD), Inter-Symbol Interference (ISI), Periodic Jitter (PJ), and Bounded Uncorrelated Jitter (BUJ) depending on the jitter source models such as Electromagnetic Interference, Cross-Talk, Bandwidth Limitation, etc. ISI and DCD are referred to as data correlated jitter. RJ, PJ, and BUJ are referred to as data uncorrelated jitter [1]-[3].

Digital serial data must be transmitted at high speeds in ATE digital test systems. A typical data rate is 200psec/bit cell. Transmission paths of the digital data are different. Some of the lines are incorporated in printed circuit board etch, and some of the lines are differential cables. Typical transmission path lengths are around 4ns in term of delay and length. The transmission path is fairly lossy at the data rate specified.

Because of stubs and impedance mismatches the transmission paths have fairly long step response, and this transient response introduces jitter. The step response might be approximated by the three-pole response as shown in Figure 1. Other interfering signals may be present near the transmission path and may inject normal-mode signal into the differential driver inputs. The purpose of the paper is to investigate how the increase in jitter can be predicted as a function of different transient responses, adjacent-line injection, and spurious signal coupling.

Although some papers have been published on this jitter model for the serial data path, they usually presented mathematical jitter model and comparison to the measurement of ATE [4][5]. In this paper, a new jitter analysis for transmission path is proposed along with Matlab and Hspice results, and presents the effect of DDJ on other jitter subcomponents.

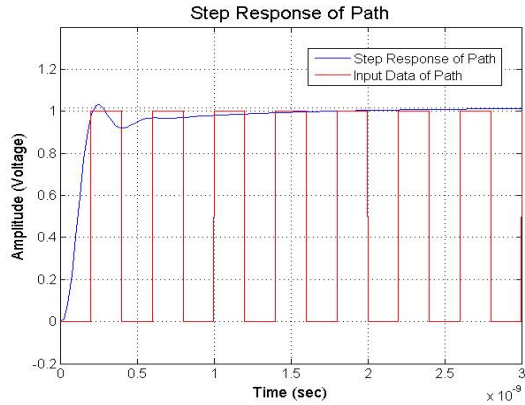


Figure 1. Step Response of Serial Data Path

The remainder of this paper is organized as follows. Section 2 shows DDJ definition, analysis, and modeling of each subcomponent in the DDJ. Section 3 presents measurement experiments followed by conclusions in Section 4.

2. Data Dependent Jitter (DDJ)

DDJ is a part of Deterministic Jitter (DJ), and consists of DCD and ISI. This is referred to as data correlated jitter, and it is simply characterized by frequency bandwidth limited model or transmission line. The response is determined by both current state and previous state of data [4][5].

2.1. Duty-Cycle Distortion Model

DCD results in high bit cells having a different width from low bit cells. It can be caused by difference in propagation delay between low to high transitions and high to low transitions. The sources of DCD can be amplitude-offset errors, turn-on delays, and saturation. Figure 2 shows the conceptual DCD model to change the duty cycle in a signal. In the DCD model, the LPF generates the bandwidth limited signal having the different high and low transition. In the comparator, threshold voltage as a controlling variable changes the pulse width for high and low logic values. The final output data is a square wave as the ideal input but has a non-50% duty cycle. The DCD PDF (Probability Density Function) is represented by two δ function and the magnitude of each function is 0.5 as shown in Figure 3. Therefore, as a heuristic approach, DCD is considered as a shift in time of the rising and falling edge. In the heuristic model, only two variables are needed to represent the shift of threshold crossing time of rising and falling transition, and samples of the discrete input data are moved by the two variables.

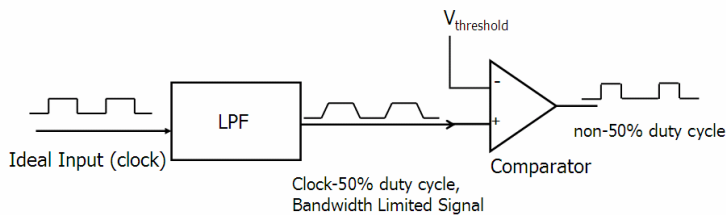


Figure 2. DCD model

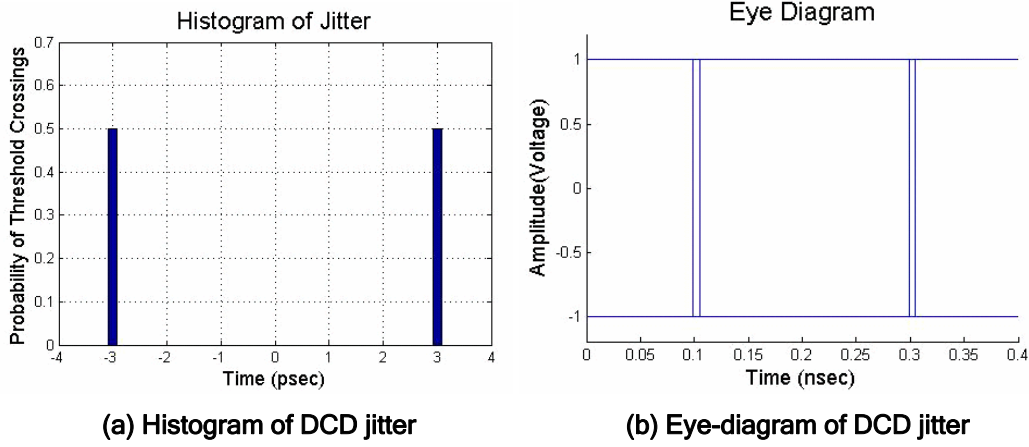


Figure 3. Example of DCD simulation

2.2. Low-Pass Filter model for ISI

ISI comes from dispersions of signals by attenuation and reflection of transmission media. The amount of ISI is dependent on high and low length in a data pattern, data rate, settling time of LFP step response, and frequency bandwidth (or edge transition time) of the data. [6] shows that edge transition time of a data was a function of the data patterns and high and low length in the data pattern. In [7], 2-pole test path model and 1-pole DUT model is suggested and the settling time of LPP step response is simply pointed out. However, the relationship between the edge transition time and ISI model and between pole location and ISI jitter have not been addressed.

Our ISI model is a LPF (Low-Pass Filter) with bandwidth limiting effect and ringing. Figure 4 shows the block diagram of the proposed ISI model. The first 1-pole LPF is a simple model for edge transition of input data. The second 3-pole LPF represents a simple DUT (Device Under Test) consisted of 1-pole, and media such as connector and cable consisted of 2-poles.

The edge transition time (T_r) of the bandwidth limited data is inversely proportional to the pole location or -3dB bandwidth of the path model [8], and it is given by

$$T_r = \frac{0.35}{f_{-3dB}} \quad (1)$$

where f_{-3dB} is -3dB bandwidth frequency, and T_r is edge transition time(10-90% of the transition time).

In the model, the input is Pseudo-Random Binary Sequence(PRBS)-7 with 5G bits/sec. In order to change the edge transition time of input data, the pole location (-3dB bandwidth) of the edge transition model is changed from 5GHz to 27GHz as shown in Figure 4.

-3dB bandwidth of the second 3-pole LPF is 20GHz. The first two-pole locations of the pole system are imaginary at $(-7.85 \pm 18i)$ GHz, and the damping ratio is 0.4 for under-damping response and ringing effect. The other is a real pole, at 16GHz. In the model, three peak-to-peak jitters are measured between A and B(1-Pole Jitter), B and C(3-Pole Jitter), and A and C(Total Jitter) as shown in Figure 4.

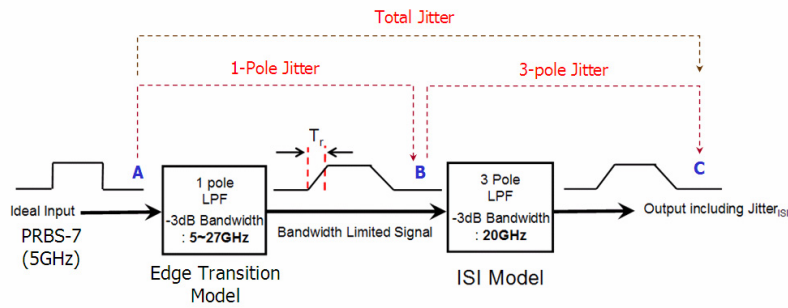
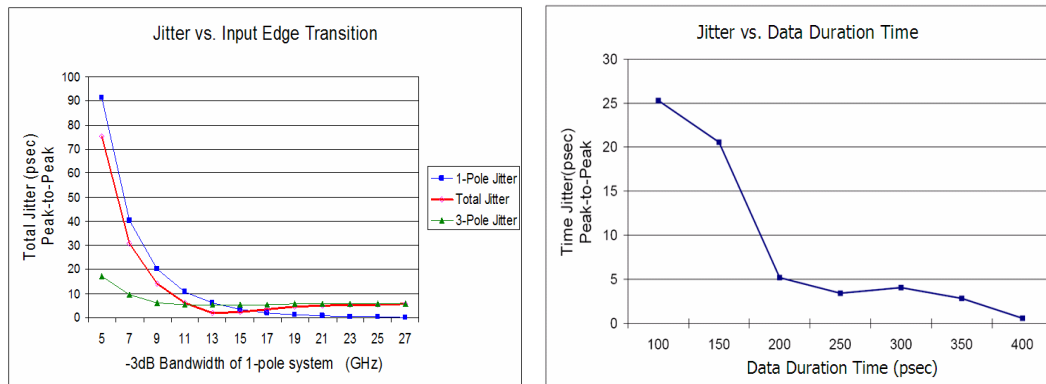


Figure 4. Block diagram of ISI model



(a) Jitter vs. Input Edge Transition

(b) Jitter vs. data duration time

Figure 5. ISI simulation

The dependency of jitter on -3dB bandwidth of data edge transition and data duration time is shown in Figure 5. As -3dB bandwidth of data edge transition decreases (edge transition time increases) in Figure 5(a), Total Jitter is more dependent on the edge transition model, i.e. if the pole-location of the 1-Pole LPF is smaller than about 20GHz, Total Jitter starts to approach the amount of 1-Pole jitter. The effect clearly shows that if -3dB bandwidth of input signal is smaller than it of ISI model, Total Jitter and 3-pole jitter is dependent on the bandwidth limited input signal. Therefore, the measured 3-Pole jitter in the model is different from the injected 3-Pole jitter. On the contrary, if the -3dB bandwidth is greater than that of ISI model, both the TJ and 3-pole jitter approach the injected ISI jitter. The above result represents that an input with some edge transition time (in this simulation, more than about 10 % of data duration time, 200psec) contributes longer edge transition time to the output of 3-pole LPF. As a result, it causes relatively shorter high and low length in the data pattern, and the shorter length makes TJ and 3-pole jitter increase. Figure 5 (b) shows more clearly the effect of the high and low length in a data pattern. It represents the relationship between jitter and data duration time. As the data duration time increases, the reflections caused by impedance mismatches of the data path become more significant, and also the edge transition time is longer than the data duration time. The effect causes more attenuation and jitter of input signal. In order to standardize the measurement of ISI jitter, the -3dB bandwidth of the input signal is greater than that of ISI model.

Figure 6 shows the effect of the pole location on ISI jitter. Peak-to-peak jitter has been used to represent the amount of ISI jitter. However, even though the peak-to-peak

jitter (5psec) is the same, the pole locations of 3-pole LPF are different and also damping ratio is changed as shown in Figure 6(a). The damping ratio is related to the settling time of LPF step response, and the relationship is given by

$$Settling\ Time = \frac{1}{2 \times damping\ ratio} \quad (2)$$

It shows that the settling time can change ISI jitter as shown in [7]. Figure 6(b) represents that if the damping ratio is fixed to 0.4, ISI jitter increases as the imaginary and real pole locations shift to the lower frequency which means the slow decay and small ringing of LPF step response increases the ISI jitter.

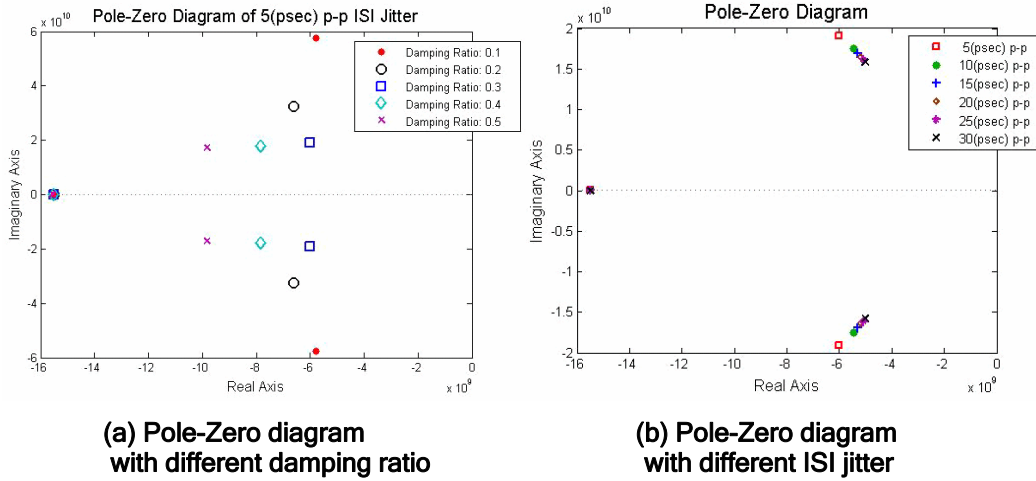


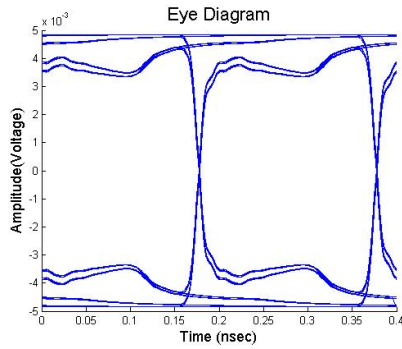
Figure 6. Pole-Zero diagram of ISI model

2.2. Transmission path model for ISI

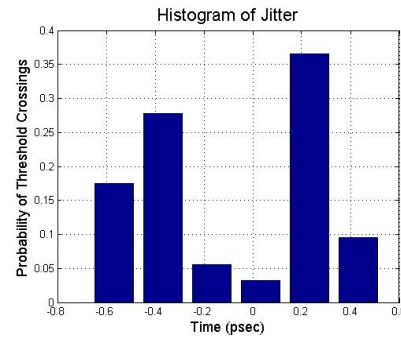
Physical media induce two main jitter sources. The first is the reflection by impedance mismatching at termination causing signal distortions. The reflection is dominated by characteristic impedance (Z_0) and reflection coefficient (Γ) including input impedance (Z_S) and load impedance (Z_L) of the transmission line [9].

In our simulation using W-model in Hspice, the path model is a 50 ohm (Z_0) coaxial cables with 100 Mhz bandwidth and 5.3dB attenuation, and the input signal is Pseudo-Random Binary Sequence (PRBS)-7 signal with 1nsec data rate. In our simulation, the signal distortion is significant and the amount of jitter increases when the reflection coefficient is negative in both the input and output nodes of the transmission, i.e. $Z_S < Z_0$, $Z_0 > Z_L$. In Hspice model, RLGC value of distributed or lumped line can be changed in order to control DDJ in data path.

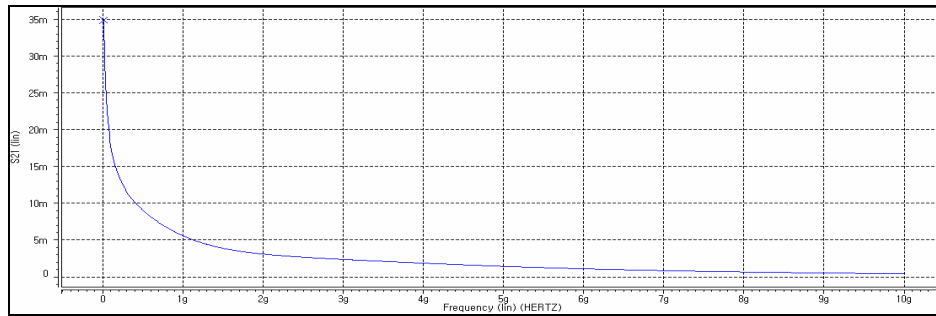
Secondly, high-frequency losses caused by skin effect and dielectric loss also affect ISI. The skin effect is proportional to the square root of the frequency, and dielectric loss is proportional to frequency [9]. Therefore, the skin effect dominates data loss at lower frequency, whereas the dielectric loss dominates at higher frequency. It's assumed that the data path is a microstrip line with 50 ohm characteristic impedance, input impedance is 10 ohm, and output impedance is 10 ohm. Input data is an ideal PRBS, and is 2,540 bits, i.e. the number of PRBS-7 pattern is 40. The data rate is 200psec.



(a) Eye-diagram



(b) Histogram



(c) S21 vs. Frequency

Figure 7. Simulation results of a microstrip path

Figure 7(a) shows the eye-diagram for transmission line, and Figure 7(b) represents the histogram of the jitter. The eye-diagram shows the attenuation in data amplitude is too big, which comes from skin effect and dielectric loss. Figure 7(c) represents S-parameter for the output of transmission path, which means the data is influenced by the frequency.

3. DDJ Experiments

In this section, experimental set up for DDJ is presented and the dependence of ISI on other jitter subcomponents is described.

3.1. DDJ Modeling Specification

In our experiment, Matlab and Hspice in PC are used to measure DDJ and combine the jitter with other jitter subcomponents. Input data is an ideal square wave, and is 2,540 bits, i.e. the number of Pseudo-Random Binary Sequence (PRBS)-7 pattern is 40. The clock frequency of clock generator is 10GHz, the bit rate of the data pattern generator is 200psec (5GHz), and the sampling rate is 1,000/bit. Three-pole Low-Pass Filter (LPF) is used to generate ISI. The LPF system consists of 2-poles and 1-pole systems. The pole locations are changed to generate the different amount of jitter, but damping ratio is always 0.4 for the under-damping response. Figure 8 is the proposed basic jitter combining method, in which ISI model is combined only one by one with another jitter component.

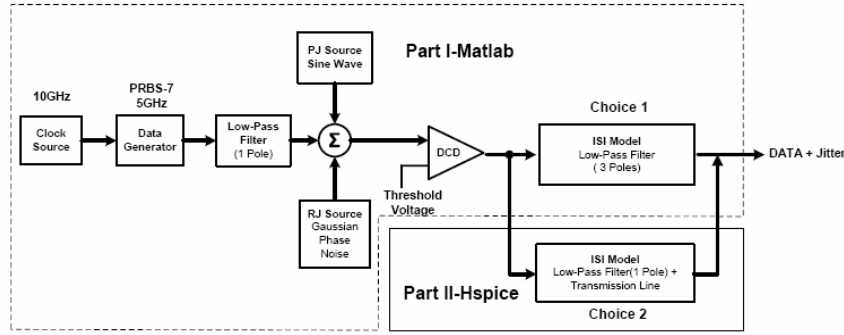


Figure 8. Basic combining method for jitter

3.2. ISI and RJ Measurement

The first experiment demonstrates the dependency of ISI on RJ. In this experiment, the Tailfit algorithm [10] is used to separate ISI and RJ. The peak-to-peak value of TJ is given by

$$\begin{aligned}
 Jitter_{total_p-p} &= Jitter_{DJ} + 14.069 \times Jitter_{RJ_RMS} \\
 Jitter_{DJ} &= a - b \\
 Jitter_{RJ_RMS} &= \frac{\sigma_a + \sigma_b}{2}
 \end{aligned} \tag{3}$$

where $Jitter_{DJ}$ is the deterministic jitter, and $Jitter_{RJ_RMS}$ is the rms value of the RJ. The RMS value of the jitter is standard deviation of the jitter.

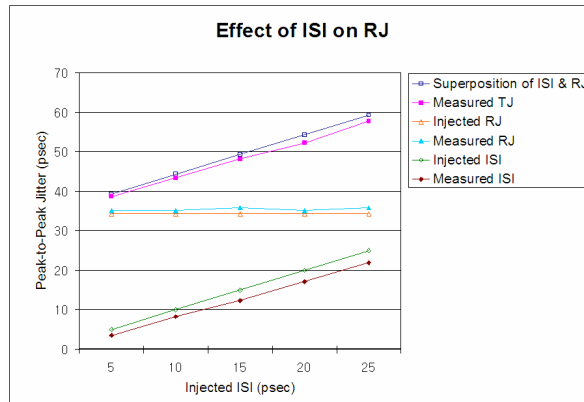


Figure 9. Effect of ISI on RJ

Figure 9 shows the effect of ISI on RJ. In this experiment, RJ is fixed to 2.44psec rms and 34.33psec peak-to-peak whereas the ISI is changed from 5psec to 25psec peak-to-peak. The results presented that the measured TJ is almost the same as the superposition of ISI and RJ. However, the measured RJ is a little greater than the injected RJ, while the measured ISI jitter is a little smaller than the injected ISI. To be exact, ISI has a little effect on RJ within 10% difference i.e. RJ is increased and ISI is decreased when ISI and RJ are combined. Therefore, the measured TJ is almost the same as the superposition of ISI and RJ.

3.3. ISI and PJ

The second experiment shows the effect of ISI changing from 5psec to 30psec peak-to-peak on PJ fixed to 15psec peak-to-peak. Figure 10 presents the result of the case where the ISI have no effect on PJ, i.e. the amount of measured TJ is the same as the superposition of ISI and PJ. And also the TJ is the same as the summation of PJ and ISI although PJ varies and ISI is fixed.

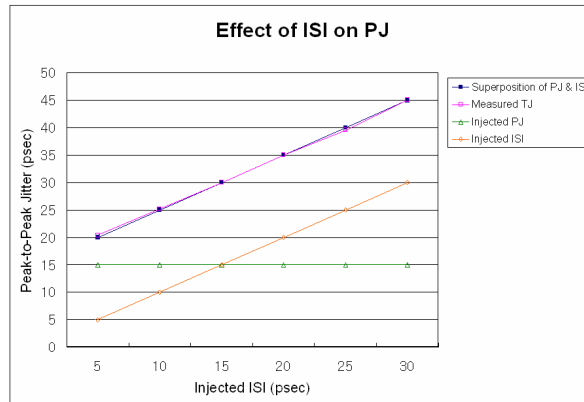


Figure 10. Effect of ISI on PJ

3.4. ISI and DCD

Finally, ISI and DCD are combined. These two jitter components are included in DJ, therefore the dependency between the two might be expected. Two different experiments are performed to look into the relationship between the TJ and the superposition of ISI and DCD. The first experiment is for a fixed DCD (15psec peak-to-peak) and a varying ISI (from 5psec to 30psec peak-to-peak). In this case, TJ is about 2psec peak-to-peak smaller than the superposition of ISI and DCD, and the value (2psec) changes very little even though the injected ISI changes as shown in Figure 11. The difference between the measured TJ and the superposition of RJ and ISI is within 5%. Therefore, the effect of ISI on DCD can be ignored.

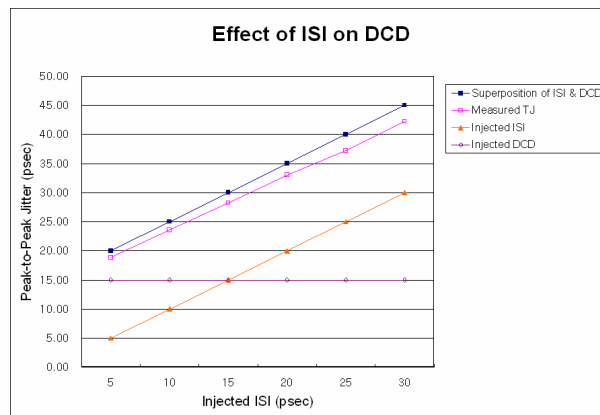


Figure 11. Effect of ISI on DCD

The second experimentation is for a fixed ISI (20psec peak-to-peak) and a varying DCD (from 5psec peak-to-peak to 30psec peak-to-peak). In this experiment, the difference between the measured TJ and the superposition of ISI and DCD is increased as the DCD increases.

Especially, when DCD is 50psec, the difference is over 10% as shown in Figure 12. This means ISI is impacted by DCD. However, since the typical DCD jitter is smaller than ISI jitter, it can be told that the superposition applies to the combining of ISI and DCD.

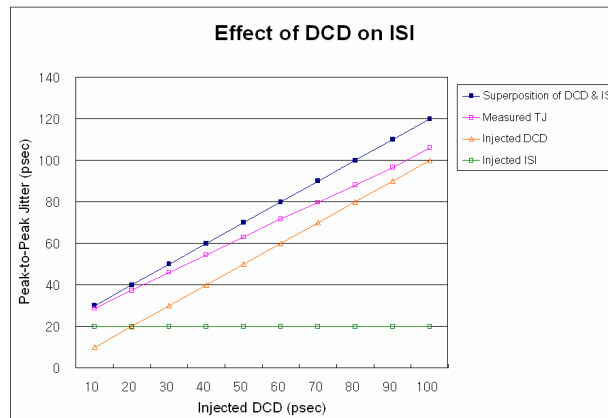


Figure 12. Effect of DCD on ISI

4. Conclusion

This paper has developed models of DDJ using Matlab and Spice, and analyzed the DDJ. DDJ was dependent on the data pattern, data rate, and data slew as well as frequency bandwidth, impedance mismatch, and loss of the data path of ATE.

In LPF model for ISI, the relationship between data bandwidth and ISI jitter was demonstrated. In addition, the transmission model for ISI was introduced and analyzed.

Finally, the dependence of ISI on other jitter subcomponents was illustrated. This will be very useful in developing and characterizing the DDJ. At the same time, this paper will be a cornerstone in standardization of jitter measurement.

5. References

- [1] "Jitter Analysis Techniques for High Data Rates," Agilent Technologies Inc., Application Note 1432, February 2003; <http://cp.literature.agilent.com/litweb/pdf/5988-8425EN.pdf>.
- [2] Wavecrest Corp., "Understanding Jitter," application note, 2001; http://www.wavecrest.com/technical/VLSI_6_Getting_Started_Guides/6understanding.PDF
- [3] Nelson Ou, Touraj Farahmand, et al., "Jitter Models for the Design and Test of Gbps-Speed Serial Interconnects," IEEE Design and Test of Computers, vol. 21, Jul-Aug 2004.
- [4] James Buckwalter, Behnam Analui, "Predicting Data-Dependent Jitter", IEEE Transactions on Circuits and Systems, Vol. 51, No. 9, Sep. 2004.
- [5] James Buckwalter, Behnam Analui, et al., "Data-Dependent Jitter and Crosstalk-Induced Bounded Uncorrelated Jitter in Copper Interconnects", Proc. IEEE International Microwave Symposium, June 2004
- [6] Takahiro J. Yamaguchi, Mani Soma, et. "Effect of Deterministic Jitter in a Cable on Jitter Tolerance Measurements.", IEEE International Test Conference, page 58-66, 2003
- [7] Jie Sun, and Mike Li, "A Generic Test Path and DUT Model for DataCom ATE", IEEE International Test Conference(ITC), Vol. 1, page 528-536, 2003
- [8] Masashi Shimanouchi, et. "New Paradigm for Signal Paths in ATE Pin Electronics are Needed for Serialcom Device Testing.", IEEE International Test Conference, page 903-912, 2002
- [9] Howard W. Jonson, Martin Graham, "High-Speed Digital Design-A Handbook of Black Magic." PTR Prentice-Hall, 1993.
- [10] Mike P.Li, Jan Wilstrup, et, "A New Method for Jitter Decomposition Through Its Distribution Tail Fitting." IEEE International Test Conference, pp788-794, 1999